Attributing the hydrological impact of different land use types and their long-term dynamics through combining parsimonious hydrological modelling, alteration analysis and PLSR analysis

Gebremicael, T.G.; Mohamed, Y.A.; Van der Zaag, P.

DOI
10.1016/j.scitotenv.2019.01.085

Publication date
2019

Document Version
Final published version

Published in
Science of the Total Environment

Science of the Total Environment 660 (2019) 1155–1167

Contents lists available at ScienceDirect

Science of the Total Environment

journal homepage: www.elsevier.com/locate/scitotenv

Attributing the hydrological impact of different land use types and their long-term dynamics through combining parsimonious hydrological modelling, alteration analysis and PLSR analysis

T.G. Gebremicael [a,b,c,*], Y.A. Mohamed [a,b,d], P. Van der Zaag [a,b]

[a] IHE Delft Institute for Water Education, P.O. Box 3015, 2601 DA Delft, the Netherlands
[b] Delft University of Technology, P.O. Box 5048, 2600 GA Delft, the Netherlands
[c] Tigray Agricultural Research Institute, P.O. Box 492, Mekelle, Ethiopia
[d] Hydraulics Research Center, P.O. Box 318, Wad Medani, Sudan

HIGHLIGHTS

- Tekeze-Atbara basin is known for its severe land degradation before the recent success in integrated watershed management.
- Combining parsimonious hydrological modelling, alteration and PLSR analysis were used to understand hydrological response.
- Expansion of agricultural resulted in an increased surface runoff and decreased dry season flow in the Geba catchment.
- This study applied a promising approach to understand impact of environmental change on the hydrology.

GRAPHICAL ABSTRACT

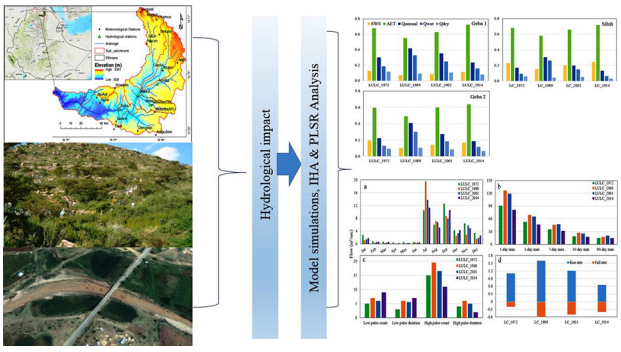

ARTICLE INFO

Article history:
Received 17 October 2018
Received in revised form 17 December 2018
Accepted 8 January 2019
Available online 09 January 2019

Editor: Ouyang Wei

Keywords:
Hydrological processes
Land use/cover
Wflow model
Geba catchment
IHA analysis
PSLR analysis

ABSTRACT

Understanding the relationship between hydrological processes and environmental changes is important for improved water management. The Geba catchment in Ethiopia, forming the headwaters of Tekeze-Atbara basin, was known for its severe land degradation before the recent success in integrated watershed management. This study analyses the hydrological response attributed to land management change using an integrated approach composed of (i) simulating the hydrological response of Land Use/Cover (LULC) changes; (ii) assessing the alteration of streamflow using Alteration of Hydrological Indicators (IHA); and (iii) quantifying the contribution of individual LULC types to the hydrology using Partial Least Square Regression model (PLSR).

The results show that the expansion of agricultural and grazing land at the expense of natural vegetation has increased the surface runoff 77% and decreased dry season flow by 30% in the 1990s compared to 1970s. However, natural vegetation started to recover from the late 1990s and dry season flows increased by 16%, while surface runoff declined by 19%. More pronounced changes of the streamflow were noticed at sub-catchment level, mainly associated with the uneven spatial distribution of land degradation and rehabilitation. However, the rate of increase of low-flow halted in the 2010s, most probably due to an increase of water withdrawals for irrigation. Fluctuations in hydrological alteration parameters are in agreement with the observed LULC change. The PLSR analysis demonstrates that most LULC types showed a strong association with all hydrological components.

* Corresponding author at: IHE Delft Institute for Water Education, P.O. Box 3015, 2601 DA Delft, the Netherlands.
E-mail address: t.gebremicael@un-ihe.org (T.G. Gebremicael).

https://doi.org/10.1016/j.scitotenv.2019.01.085

These findings demonstrate that changing water conditions are attributed to the observed LULC change dynamics. The combined analysis of rainfall-runoff modelling, alteration indicators and PLSR is able to assess the impact of environmental change on the hydrology of complex catchments. The IHA tool is robust to assess the magnitude of streamflow alterations obtained from the hydrological model while the PLSR method is useful to zoom into which LULC is responsible for this alteration.

1. Introduction

Understanding variability and change of hydrological processes and their implications on water availability is vital for water resource planning and management. Human-induced environmental changes are key factors controlling the variability of streamflow (Hassaballah et al., 2017; Woldesenbet et al., 2017). Excessive pressure on land resources aimed at providing food, water and shelter have resulted in a significant change of land cover which consequently modified the hydrological regimes (Gyamfi et al., 2016; Savenije et al., 2014). Alteration of existing land management practices in a catchment affects the hydrological processes such as infiltration, groundwater recharge, base-flow and surface runoff and consequently the overall water availability in rivers (Hurkmans et al., 2009; Kiptala et al., 2013). The Land Use/Land Cover (LULC) changes significantly influence the timing and magnitude of extreme events (Woldesenbet et al., 2017; Yan et al., 2016). As such, the effect of LULC change on hydrology has continuously drawn the attention of scientific communities to understand the complex relationship between hydrological processes and human-induced environmental changes. However, the heterogeneity of catchment characteristics coupled with limited hydro-climatological data is the major scientific challenge to fully understand such complex relationships (Gashaw et al., 2018; Gyamfi et al., 2016; Li and Sivapalan, 2011; Tekleab et al., 2014).

The Ethiopian highlands, covering 45% of the country, is affected by severe LULC and land degradation problems (Gashaw et al., 2018; Haregeweyn et al., 2014; Nyssen et al., 2014). Because of the high increase of population, a rapid expansion of cultivable lands has significantly reduced land with natural vegetation (Ariti et al., 2015; Gebremicael et al., 2013 & 2018; Haregeweyn et al., 2017; Hurni et al., 2005). Zeleke and Hurni (2001) reported an increase of cultivable land by 77% (1957–1995) in the Dembecha watershed of the Blue Nile basin and a decline of forest coverage by 99%. Haregeweyn et al. (2014) showed that agricultural land in the Gilgel Tekeze watershed increased by 15% at the expense of shrubland which decreased by 19% between 1976 and 2003. In contrast, Wondie et al. (2011) revealed that forest coverage in the Semen mountain national park of the Blue Nile basin increased by 33% in 20 years. These changes can modify water resources availability in those catchments as it affects the partitioning of rainfall into different hydrological components (Taniguchi, 2012). A number of studies investigated impacts of LULC change on the hydrology at different spatiotemporal scales (Chen et al., 2016; Gebremicael et al., 2013; Hassaballah et al., 2017; Tekleab et al., 2014; Woldesenbet et al., 2017). However, the results indicated that the impacts are not universal as it depends on the local context of the specific catchment (Gebremicael et al., 2018; Haregeweyn et al., 2014). While some studies show that the conversion of human-modified land cover back to natural vegetation cover reduces surface runoff while enhancing the base-flow (Chen et al., 2016; Haregeweyn et al., 2014), other studies showed that increased natural vegetation cover reduces runoff as more of the incoming rainfall is contributed to canopy interception and evapotranspiration (Ott and Uhlenbrook, 2004; Wang et al., 2018).

The Tekeze-Atbara headwaters located in Ethiopia, which is one of the sources of the Nile water, is characterized by severe land degradation. The natural vegetation has been replaced by cultivable and grazing lands during the period of the 1960s to the early 1990s (Belay et al., 2014; Tesfaye et al., 2017). Nevertheless, forestation started to recover from the late 1990s due to watershed management interventions (Belay et al., 2014; Nyssen et al., 2010). Local studies revealed that the impact of LULC on the hydrology of the basin is significant. Abraha (2014) reported that the conversion of natural vegetation to agricultural crops in the upper Geba catchment increased surface runoff by 72% and decreased dry season flow by 32% over 1972–2003. In contrast, Bizuneh (2013) found that despite almost all land had been converted into cultivable area, the response of surface runoff and base-flows did not change in the Siluh watershed, located in the same region. The disagreement suggests the impact of LULC on the hydrological processes is site-specific and varies with catchment scale. As such, it is necessary to investigate the space-time relationship between LULC and hydrological responses to support informed land and water management interventions.

The effect of LULC change on hydrological processes has been studied using ground measurements, hydrological models, multivariate statistics and paired catchment methods (Gashaw et al., 2018; Kiptala et al., 2014; Shi et al., 2013). Hydrological models, ranging from conceptual to fully physically based distributed models have been applied in different regions. These types of models have their own advantages and disadvantages (Savenije, 2010). The fully distributed physical models are appropriate to accurately describe the hydrological process in a complex catchment (Savenije, 2010; Wang et al., 2016). However, the excessive complexity of models (over-parameterization) makes model calibration extremely challenging (Savenije, 2010; Uhlenbrook et al., 2004). The over-parameterization problem is not the primary concern of conceptual models, but they usually fail to reproduce the nonlinear dynamics of catchment characteristic which is essential in studying the hydrological response to the dynamics of environmental changes (Sivapalan et al., 2003). Therefore, to avoid over-parameterization and maximize information retrieved from spatial data, this study attempted to develop a parsimonious dynamic distributed model which requires modest calibration. The literature shows that PCRaster/Python programing language are becoming popular tools to develop dynamic and flexible distributed hydrological models, such as Wflow and TOPMODEL (Karssenberg et al., 2010; Wang et al., 2016). The spatially distributed hydrological models have the potential of simulating the impact of human-induced environmental changes. In this study, a spatially distributed hydrological model based on the Wflow-PCRaster/Python modelling framework was developed to simulate the hydrological processes. The Indicators of Hydrological Alteration (IHA) Model (Mathews and Richter, 2007) was applied to assess the degree of streamflow alterations. The contribution of individual LULC changes on the hydrological components was then investigated using a Partial Least Square Regression (PLSR) model (Abdi, 2010). The IHA tool is robust to assess the magnitude of streamflow alterations obtained from the hydrological model while the PLSR method is useful to zoom into which LULC is responsible for this alteration.

2. Description of study area

This study was carried out in the Geba catchment (Fig. 1), located in the northern part of Ethiopia, extending from 38°38′ to 39°48′E and 13°14′ to 14°16′N and draining an area of 5085 km^2 (Gebremicael et al., 2018). It forms the headwaters of the Tekeze-Atbara (T-A) river basin, one of the major tributaries of the Nile River. The topography is generally characterized by highlands and hills in the north and north-

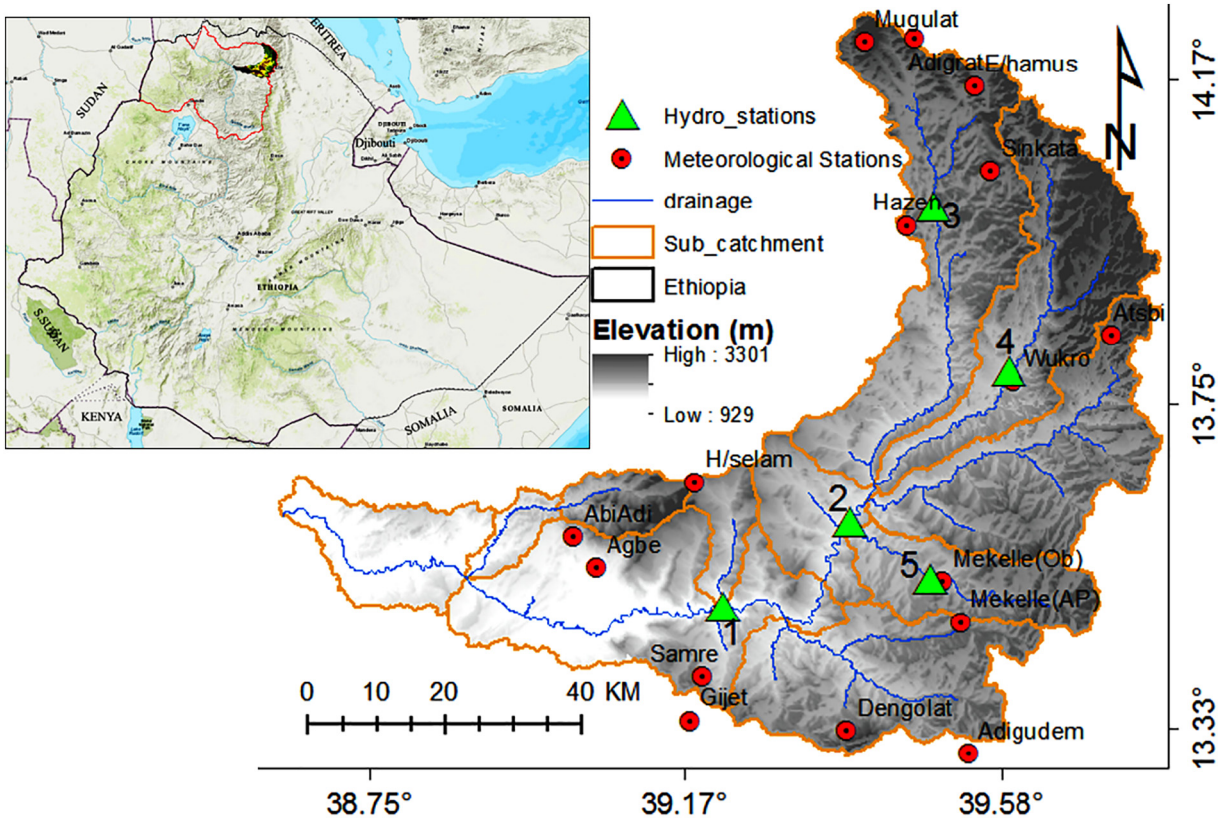

Fig. 1. Location of the study area, meteorological and hydrological monitoring stations.

east and plateaus in the central part of the catchment. The elevation of the Geba catchment ranges from 930 m.a.s.l. at the outlet to 3300 m.a.s.l. at the Mugulat Mountains near the city of Adigrat (Fig. 1). The catchment has four main sub-catchments: Siluh, Genfel, Illala and Agula. Siluh (960 km^2) sub-catchment drains the Mugulat Mountains in the northern part of Geba, with annual rainfall varying between 500 in the lower valley to >650 mm/year in the highland areas near E/hamus and Mugulat (Fig. 1). Similarly, Agula (481 km^2) sub-catchment is characterized by highly dissected and rugged terrains with elevations varying from 1750 m.a.s.l. at the confluence with the Geba, to 2800 m.a.s.l. in the mountains near Atsbi town, with a high rainfall variability, ranging from 450 to 700 mm/year. The Genfel (730 km^2) sub-catchment is located in-between Siluh and Agula sub-catchments, with an elevation range from 1780 m.a.s.l. at the confluence with Siluh, 7 km upstream of Geba2 gauging station in the Geba river, to >2800 m.a.s.l. in the Atsbi highlands. The fourth sub-catchment is Illala (340 km^2), which drains an area of 340 km^2 and joins the main Geba River at 2 km downstream of the Geba2 gauging station. Unlike in the earlier sub-catchments, this sub-catchment is dominated by flat areas where agriculture and settlements are the major land cover. The largest city (Mekelle) in northern Ethiopia is found within this sub-catchment. The rainfall over this catchment is very erratic in distribution and magnitude with an annual average below 550 mm/year. Further down the Geba river is joined by smaller tributaries.

The catchment is characterized by a semi-arid climate, the majority of rainfall occurring from June to September. >70% of the total annual rainfall is falling with high storm intensities during only 2 months (July and August) (Gebremicael et al., 2017). The high variability of rainfall is linked to the seasonal migration of the intertropical convergence zone (ITCZ) and the rugged topography of the area (Nyssen et al., 2005).

According to Gebremicael et al. (2018), the present LULC in the study area is composed of agriculture (39%), bush and shrubland (30%), bareland (11%), grassland (7%), wooded land (6%), natural forest (1.7%), forest plantations (3.8%), settlements (1.2%), and water bodies (0.3%). Detailed descriptions and analysis of those LULC types are found in Gebremicael et al. (2018). Although rain-fed agriculture is the most common source of food production in the catchment, small-scale irrigated agriculture has significantly increased in the last 10 years (Gebremeskel et al., 2018). Rain-fed agricultural and bareland areas have intensified at the expense of natural vegetation cover. However, since the mid-1990s, the rate of deforestation has decreased, land degradation largely halted and the area with natural vegetation started to increase again after watershed management interventions. Various forms of watershed management programs have been implemented in the last two decades (Belay et al., 2014; Gebremeskel et al., 2018). Accordingly, water availability has increased in the previously degraded lands (Gebremeskel et al., 2018; Nyssen et al., 2010).

Geological formations of the catchment include Enticho Sand stone, Edag Arbai Tillites, Adigrat Sandstone, Antalo Super sequence and Metamorphic rocks (Gebreyohannes et al., 2013). Clay loam (40%), sandy clay loam (30%), clay (19%), loam (10%), and sandy loam (1%) are the dominant soil texture classes in the area (Gebreyohannes et al., 2013). Soil textures in the catchment are deeply weathered in the uppermost plateaus, rocky and shallow soils in the vertical scarps, coarse and stony soils on the steep slopes, finer textured soils in the undulating pediments and most deep alluvial soils are found in the alluvial terraces and lower parts of the alluvial deposits (Gebreyohannes et al., 2013). The depth of soils in the catchment is limited due to contagious hard rocks and cemented layers.

3. Data and methods

3.1. Data inputs

This study employed temporal (Precipitation and Evapotranspiration) and spatial (Digital Elevation Model (DEM), Soil, LULC) datasets to develop distributed hydrological models. These datasets are explained in detail in the following paragraphs.

Land Use/Land cover (LULC), Digital Elevation Model (DEM), soil type, Local Drainage Direction (LDD) and river maps are required to develop a distributed hydrological model in a Wflow_PCRaster/Python framework environment (Schellekens, 2014). The land cover dataset may not be completely static, but assumed static for a given model simulation. The four models have four different LULC maps, but each map is static for the given model. LULC data of the catchment were acquired from our previous study (Gebremicael et al., 2018). In that study, Landsat images of the years 1972, 1989, 2001, and 2014 for the Geba catchment were processed. The years for analysis were selected based on key signs of LULC change (land degradation, land policy changes and availability of the satellite image). An intensive field data, including ground truth (3326 points), interviews and observations, topographic maps, aerial photographs and secondary information from the literature were used to validate the land use classification. A hierarchical classification comprised of unsupervised/supervised approaches was performed to identify nine LULC class types in the catchment (Table 1). For more information about classifications and accuracy assessments, refer to Gebremicael et al. (2018). For this study, these LULC types were re-classified into seven classes where the plantation and forest, as well as bareland and urban classes, were merged as forest and bareland, respectively.

The initial soil map, available online from the International Soil Reference and Information Centre (ISRIC) SoilsGrid250 (Hengl et al., 2017), was modified based on the study area characteristics. Additionally, detailed soil properties such as texture, bulk density, available water capacity, hydraulic conductivity, saturated hydraulic conductivity, soil depth, particle-size distribution, were obtained from soil samples collected from the Geba catchment. A total of 160 soil samples, 23 per land use type and equally distributed among the sub-catchments, were collected and analysed in Mekelle soil research laboratory of the Tigray Agricultural Research Institute. Soil types from the ISRIC map were reclassified into seven major groups and the physical properties of each soil group were enhanced with the result of the 160 soil samples. A 30 m resolution DEM, used to delineate the catchment boundaries and derive the LDD, were obtained from the Shuttle Radar Topographic Mission (SRTM).

The temporal data such as daily climate data were collected from 16 stations located within and surrounding the catchment (Fig. 1). These data were provided by the National Meteorological Agency (NMA). The consistency and quality of these data were checked and screened as summarized in Gebremicael et al. (2017). Observed rainfall data from the gauging stations were spatially interpolated using the Kriging interpolation method (Oliver and Webster, 1990). Daily potential evapotranspiration (PET) was estimated using Hargreaves method which is suitable in catchments with limited climatic data (Hargreaves and Riley, 1985). Finally, all dynamic and static input maps were projected to WGS-84-UTM-zone-37 N and resampled to a resolution of 100 m for the model inputs. Hydrological flows of five gauging stations (Fig. 1) were collected from the Ethiopian Ministry of Water Resources for calibration and validation of the model. Descriptions and quality of these data are presented in Gebremicael et al. (2017).

3.2. Methods

3.2.1. Development of the hydrological model

In this study, a distributed hydrological model based on the Wflow_PCRaster/Python framework was developed to assess the impact of LULC change on streamflow dynamics. Wflow is an open source software developed by the Deltares OpenStreams project which simulates catchment runoff in both limited and rich data environments (Schellekens, 2014). Wflow_sbm model is based on TOPOG hydrological tool described in Vertessy and Elsenbeer (1999). This model was derived from the CQFLOW model (Köhler et al., 2006) and is programmed in the PCRaster-Python environment (Karssenberg et al., 2010). It was selected in this study for its improved consideration of both infiltration and saturation excess runoff generation processes. A schematized representation of Wflow_sbm is given in Fig. 2.

The hydrological processes in the model are represented by three main routines. Interception is calculated using Gash model (Gash et al., 1995) which uses PET to drive actual evapotranspiration based on the soil water content and land cover types. The Soil Water Storage (SWS) processes that control runoff generation is calculated by the TOPOG_sbm (Vertessy and Elsenbeer, 1999). TOPOG_sbm was specifically designed to simulate fast runoff processes; however, a considerable improvement has been made in Wflow_sbm to make it more widely applicable (Schellekens, 2014). Details of interception and soil model equations in Wflow_sbm are provided as supplementary files (Appendix S1 and S2). The river drainage and overland flows are modelled using kinematic wave routing. Rainfall and evaporation in the saturated canopy are calculated for each event to estimate the average rainfall and evaporation from the wet canopy. The remaining water infiltrates into the soil and when the rain falls on partially saturated soil, it directly contributes to surface runoff. At the same time, part of the soil water is taken by evapotranspiration. The infiltrated water exchanges between the unsaturated stores (U) and saturated store (S) of the soil (Fig. 2). The soil in Wflow_sbm is considered as a simple bucket model which assumes an exponential decay of the saturated hydraulic conductivity (Ksat) depending on the depth (Schellekens, 2014). The soil depth of the different land cover types in the model is identified and scaled using a topographic wetness index (Vertessy and Elsenbeer, 1999). As the model is fully distributed, the runoff is calculated for each grid cell with the total depth of the cell is divided into saturated and unsaturated zones (Fig. 2). Darcy's equation is applied in the model to simulate lateral flow from the saturated zone. The total runoff from a given catchment is the sum of surface runoff and lateral flow which is routed from the river network as discharge using the kinematic wave routing.

The hydrological process described by the different modules is represented by 19 main parameters (Table S1). These parameters are

Table 1
LULC types and their changes between the years 1972, 1989, 2001 and 2014.

Land use/cover	1972	1989	2001	2014	Change (%)			
	Area (km^2)	Area (km^2)	Area (km^2)	Area (km^2)	1972–1989	1989–2001	2001–2014	1972–2014
Agriculture	1402	1824	2111	1995	30	16	−5	42
Wood land	791	262	284	307	−67	8	8	−61
Forest land	375	145	60	78	−61	−59	31	−79
Bareland	636	1250	831	561	97	−34	−33	−12
Urban areas	1	12	31	48	1130	148	57	4680
Plantations	0	56	130	194	NA	135	49	NA
Water body	0	0	6	12	NA	3050	92	NA
Bush & shrub land	1489	1296	1376	1532	−13	6	11	3
Grass land	391	240	258	358	−39	7	39	−8

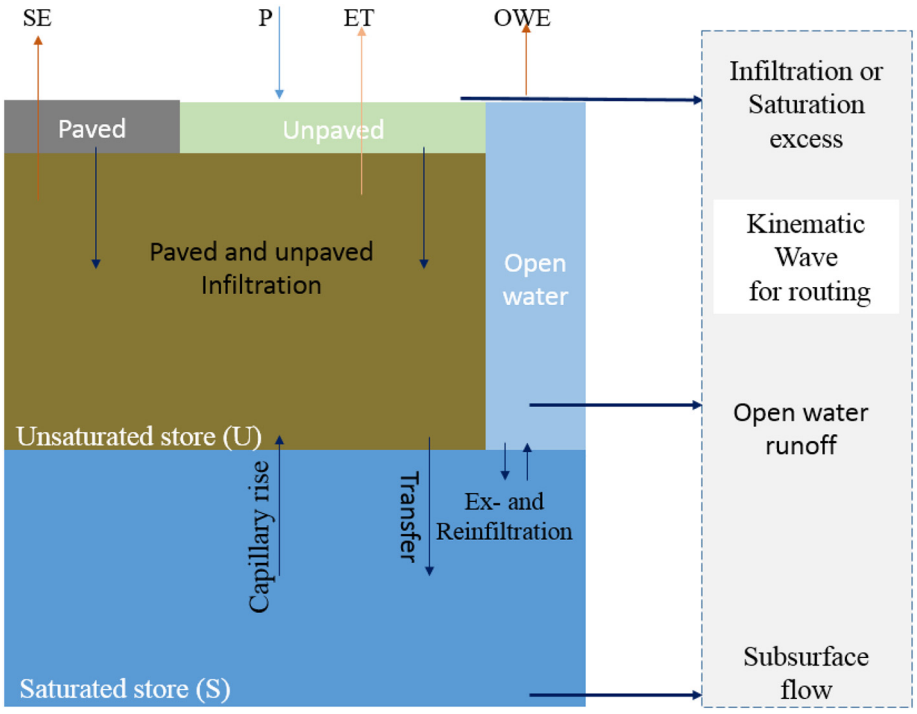

Fig. 2. Schematization of the different processes and fluxes in wflow_sbm model (modified from Schellekens, 2014). P = precipitation; SE = soil evaporation; ET = Evapotranspiration, OWE = open water evaporation.

linked to the model by a PCRaster look-up table that contains four columns. The columns are used to identify the land use type, subcatchment, soil type and the values assigned based on the first three columns, respectively.

3.2.2. Model calibration and validation

The developed models were calibrated and validated using the LULC of 2014 and 1972 for the reverse and forward modelling approaches, respectively. The 2014 model has been calibrated and validated at five locations, while two locations were used for the 1972 model, respectively. Forward modelling was done at only two stations due to the absence of streamflow data in the 1970s at three locations. First, it was calibrated and validated at Geba1 and subsequently at four smaller catchments (Fig. 1). Calibration of the model started with a selection of parameters and their initial values from the literature (Hassaballah et al., 2017; Schellekens, 2014) and our own field observations and laboratory analysis. Prior to calibration, 1 year data (2009) were used to initialize the model conditions and identify the most sensitive parameters. Next, the values of sensitive parameters were manually adjusted until maximum concordance between observed and predicted streamflow occurred. The model was then evaluated using different objective functions to verify whether the predicted and observed streamflow agreed.

The model – in fact two models, were calibrated and validated separately as follows:

1. The first model uses LULC of the year 1972, and run by observed daily datasets of climatic data (precipitation and Evapotranspiration) from 1971 to 1976. First 3 years (1971 to 1973) were used for calibration of the model against observed streamflow, while the remaining 3 years (1974 to 1976) were used for model validation.
2. The second model uses LULC of 2014, and run by observed climatic data (precipitation and Evapotranspiration) from 2010 to 2015. The first 3 years (2010 to 2012) were used for calibration of the model against observed streamflow data while the remaining 3 years (2013 to 2015) were used for model validation.

Similarly, the datasets of 2010 to 2012 and 2013 to 2015 were used for calibration and validation of the 2010s model, respectively. The two calibrated models were used to investigate the hydrological responses for each of the four LULC maps (1972, 1989, 2001 and 2014). These models and input datasets are summarized in Table 2. Nash–Sutcliffe Efficiency (NSE) and Percent Bias (PBIAS) statistical indices were applied to evaluate the performance of the model. Detailed descriptions of these indices are given in our previous study (Gebremicael et al., 2017).

3.2.3. Impact modelling approach

The two calibrated models (1972, and 2014) were applied to the classified LULC maps of 1972, 1989, 2001 and 2014 to assess the impact of LULC change on the hydrology which results in 8 model outputs (Table 2). The "fixing-changing method" that is changing LULC maps while keeping model parameters and other input datasets (hydrology, climate, soil and DEM) constant was used in a number of studies to assess the impact of LULC change on hydrological response (Gashaw et al., 2018; Gyamfi et al., 2016; Woldesenbet et al., 2017; Yan et al., 2016). As streamflow data is not available in the 1980s and early 1990s, the "fixing-change simulation method" is suitable to simulate the hydrological response attributed to LULC change in the 1980s.

First, the calibrated model using the map of 2014 was used to simulate the hydrological response of 2014, 2001, 1989 and 1972 LULC maps. Second, a similar procedure was applied to see the hydrological

Table 2
Summary of the different developed models and their input datasets.

Model name	Model parameters	Input datasets	Year of LULC	Remarks
F_1972	P_1972	1972	1972	Forward modelling
F_1989			1989	
F_2001			2001	
F_2014			2001	
R_2014	P_2014	2014	2014	Reverse modelling
R_2001			2001	
R_1989			1989	
R_1972			1972	

responses of 1972, 1989, 2001 and 2014 LULC maps using the calibrated model parameters with the 1972 LULC map. As summarized in Table 2, the same model parameters and input datasets from 2014 and 1972 models were used to simulate the hydrological responses of 2014, 2001, 1989 and 1972 LULC maps in the reverse modelling and forward approaches, respectively. Applying both reverse and forward modelling approaches is essential to minimize input data uncertainties during calibration and validation processes (Yu et al., 2018). Due to the observed dynamic change in LULC (Table 1), the value of model parameters is expected to vary during the study period. Hence, employing both reverse and forward modelling approaches is essential to conduct an in-depth analysis of the hydrological response to LULC change dynamics from both directions.

3.2.4. Application of indicators of hydrological alterations (IHA)

The change of streamflow dynamics caused by the change in LULC, as simulated by the hydrological models, was also quantified by Indicators of Hydrological Alterations (IHA). The IHA software developed by the US Nature of Conservancy (Mathews and Richter, 2007) were used to detect the hydrological fluctuations in the catchment. Characterizing these hydrologic parameters is essential to understand the variation of hydrological systems before and after environmental changes (Hassaballah et al., 2017; Saraiva-Okello et al., 2015). 33 IHA parameters were considered to characterize the (simulated) flow variations between 1972 and 1989, 1989–2001, and 2001–2014, including monthly flow condition, magnitude and timing of extreme flows, flow pulses and rates of change.

3.2.5. Partial least square regression (PLSR) analysis

Analysing hydrological responses and change using hydrological simulation and IHA analysis cannot reveal the contribution of each LULC type to hydrological change. A combined use of the hydrologic model, IHA and PLSR could be a viable approach to scrutinize the impact and contribution of each LULC change on the catchment hydrological responses. The pair-wise Pearson correlation combined with the PLSR model (Abdi, 2010) was applied to further investigate the relationship between individual LULC types and each hydrological component.

This approach is essential to ascertain whether the observed change in LULC was large enough to cause the change in streamflow dynamics. The relation between each LULC type and hydrological components was computed using the pair-wise Pearson correlation while the contribution of their change to the streamflow was quantified using the PLSR model. The PLSR is a robust multivariate regression technique that is appropriate when the response (dependent variables) exhibit collinearity with many predictors (independent) variables (Shi et al., 2013; Woldesenbet et al., 2017). It combines features from principal component analysis and multiple regressions that is appropriate when predictors exhibit multicollinearity (Yan et al., 2016). In this study, the independent variables are the different LULC types (Table 1) while the dependent variables are hydrological components (total runoff, wet and dry season flow, actual evapotranspiration (AET) and SWS). Detailed information on PLSR algorithms can be found in the literature (Abdi, 2010; Shi et al., 2013) and hence only a brief description is given here.

An interesting feature of the PLSR model is that the relationship between the independent and dependent variables can be inferred from weights (w*) and regression of each independent variable in the most explanatory components (Abdi, 2010). This is essential in order to identify which LULC is strongly associated with the streamflow. The quality and strength of the model are measured by the proportion of variance in the matrix of independent variables used in the model (R^2x), the proportion of the variance in the matrix of dependent variables explained by the model (R^2y) and cumulative goodness of prediction within a given number of factors (Q^2_{cum}). Values of R^2x, $R^2y > 0.5$ and $Q^2_{cum} > 0.097$ are considered as a good predictive ability of the model (Tenenhaus, 1998). A cross-validation was used to determine the number of significant PLSR components. Detailed information on the calculations of these indices are explained in Shi et al. (2013) and Yan et al. (2013). The importance of predictors of both independent and dependent variables of the PLSR modelling is given by the Variable Influence Projection (VIP). Predictors with higher values of VIP better explain the consequence of the independent on the dependent variables. As a rule of thumb, VIP > 1 is statistically significant to explain the dependent variables (Yan et al., 2013). Weight (w*) coefficients in the PLSR model describe the direction and strength of contributions from each independent variable (Yan et al., 2016). Small values of VIP and W* reveal that the variable is not relevant to explain the dependent variable and can be excluded from the model. To infer if the samples are given from a normally distributed population or not, normality was checked using the Shapiro and Wilk (1965) normality test. The PLSR modelling and other statistical analysis including the multicollinearity of predictors were performed with SPSS software (Carver and Nash, 2009) and XLSTAT tool (www.XLSTAT.com).

4. Results

4.1. Calibration and validation of the Wflow hydrological model

The simulated and observed streamflow in the calibration and validation periods using the 2014 and 1972 models are given in Fig. 3 (for three locations) and 4 (for two locations), respectively. Results for additional two stations for the 2014 model are given in the supplementary file (Fig. S1).

Model parameters such as saturated hydraulic conductivity (Ksat), residual water content (thetaR), CanopyGapFraction, M parameter (controls decay of hydraulic conductivity with depth), and Manning coefficient (N) were the most important parameters controlling outflow. Optimized model parameter values after the calibration processes are summarized in Tables S2–S6. Parameter values varied from sub-catchment to sub-catchment within the same calibration period and from time (1970s) to time (2010s). For example, the average value of CanopyGapFraction for all LULC types is higher in Geba2 (0.28) and Siluh (0.26) than in Geba1 (0.2) (Tables S2–S4). Similarly, the value of this parameter significantly reduced from the 1970s (0.52) to 2010s (0.25).

As presented in Figs. 3 and 4, the models were able to simulate the observed flow consistently in all gauging stations during the 2010s and 1970s calibration processes. To show that the models could reproduce the low flows, the same figures but in log scale are provided in the supplementary file (Fig. S2).

The performance indices for the daily calibration and validation are listed in Table 3. The value of NSE during calibration and validation is >0.6 with PBIAS around ±25% in three stations during the 2010s and in both stations during the 1970s comparisons (Table 3). This suggests very good model performance (Moriasi et al., 2007). The model performed relatively less in Genfel and Illala catchments with NSE of <0.6 and higher PBIAS during validation (Table 3 and Fig. S1). The positive value of PBIAS shows the tendency of the model to consistently overestimate the streamflow across all gauging stations (Figs. 3 and 4). For example, the streamflow was overestimated by 9.6%, 13.2% and 11.2% during calibration and 11.8%, 18% and 14.3% during validation in Geba1, Geba2 and Siluh stations, respectively. In contrast, peak flow in Geba1 and Siluh were slightly underestimated during 2010 and 2011, respectively. Such overestimation and slight underestimation could also be attributed to the interpolation of the sparse and unevenly distributed rain gauges over the complex terrains of the catchment. Comparing the different sub-catchments, the performance of the model slightly improved at the downstream stations (Table 3). The likely reason is that some of the errors at smaller scale counter-balanced each other when combined at downstream stations. Generally, the consistency of simulated and observed hydrographs and statistical indices indicate that the model was able to describe the daily streamflow of the

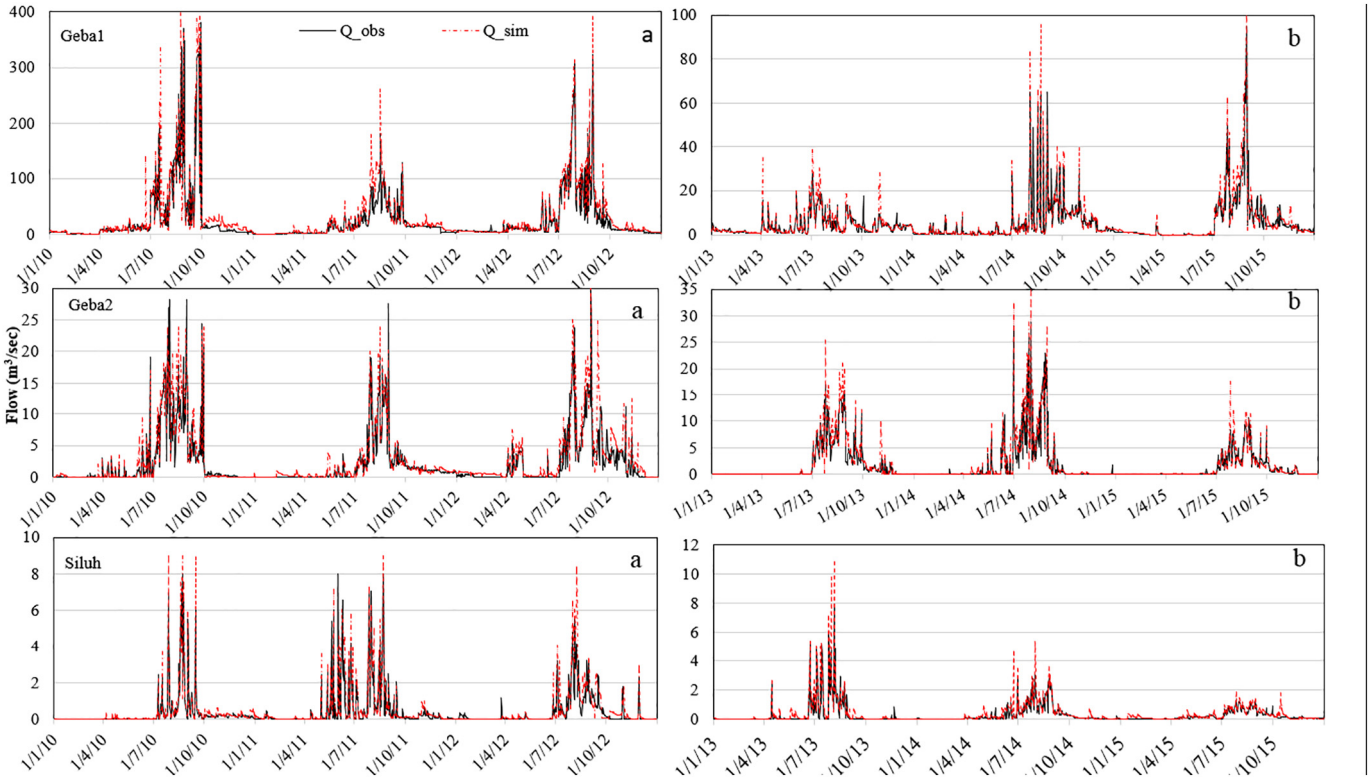

Fig. 3. Calibration (a) and validation (b) of Wflow model using LULC of 2014 in three sub-catchments of the basin.

catchment. Thus, the calibrated models in the 2010s and 1970s were applied to simulate the impact of LULC change in the catchment.

4.2. Streamflow responses to LULC changes

Figs. 5 and 6 shows streamflow of the sub-catchments simulated from LULC maps of different periods. Comparison between the hydrographs obtained from each LULC map indicated that the streamflow is significantly affected by the observed change in LULC in all sub-catchments. For example, the peak flows from the LULC map of 1989 were higher than from the remaining maps during the reverse (Fig. 5) and forward (Fig. 6) modelling approaches. Although the magnitude of peak flow from 2001 and 2014 maps is still higher than the 1972 map, it has slightly decreased compared to the 1989 LULC. In contrast, the low flows during the dry months have significantly decreased from 1972 to 1989 and started to increase from 1989 to 2001. The rate of increase of the low flows from 2001 to 2014 halted in most catchments. The results from the reverse modelling approach (Fig. 5) is in agreement with the forward modelling approach (Fig. 6) wherein both cases similar patterns of change in peak and dry season flows were observed.

During the reverse modelling approach, the total runoff from the main outlet (Geba 1) has increased by 38% from 1972 to 1989 and then decreased by 15% and 34% using 2001 and 2014 maps, respectively

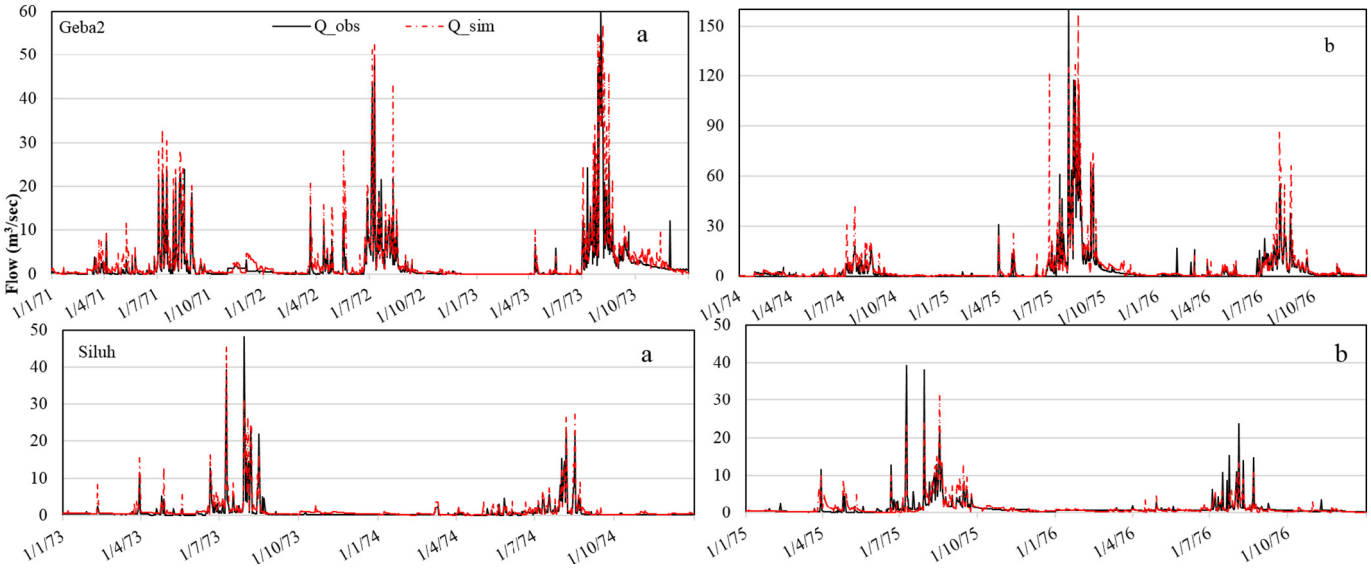

Fig. 4. Calibration (a) and validation (b) of Wflow model using LULC of 1972 in two sub-catchments of the basin.

Table 3
Performance criteria of the model calibration and validation at different monitoring stations.

Catchment	2014 model (reverse modelling)				1972 model (forward modelling)			
	Calibration		Validation		Calibration		Validation	
	NSE	PBIAS (%)	NSE	PBIAS (%)	NSE	PBIAS (%)	NSE	PBIAS (%)
Geba1	0.83	12.35	0.81	10.73				
Geba2	0.76	19.22	0.83	10.73	0.77	12.27	0.75	14.46
Siluh	0.86	15.14	0.84	21.83	0.71	24.39	0.67	18.07
Genfel	0.69	61.91	0.58	14.29				
Illala	0.55	23.94	0.49	27.72				

(Table 4). The wet season flow exhibited a similar pattern to total runoff. Contrasting to the annual and wet season flows, the dry season flow decreased by 23% and increased by 17% during the 1972–1989 and 1989–2001 periods, respectively. However, a decrease of 25% was noticed using 2014 LULC (Table 4). As with the SWS and AET fluxes, the average value of AET over the whole catchment decreased by 18% in 1989 compared to 1972 and then increased by 13% and 15% in 2001 and 2014, respectively. Similarly, SWS in soil and contribution to groundwater recharge decreased in the first period and increased during the second and third periods (Table 4). A summary of the results for the two remaining sub-catchments (Genfel and Ilala) during reverse and forward modelling (Geba2 and Siluh) are given in the supplementary file (Tables S7–8). The long-term change pattern of each hydrological component corresponding to the observed LULC change periods is also illustrated in Fig. 7. The value of each hydrological component is normalized by the mean annual rainfall.

At the sub-catchment level, more pronounced changes of hydrological flows could be noted. For example, the observed total surface runoff in 1972 at Geba2 increased by >82% in 1989 while SWS and AET decreased by >49 and 18%, respectively. Similarly, in Siluh sub-catchment, AET and SWS declined by 32% and 15%, whereas the total runoff increased by >100% for the same period. Such changes are mainly associated with the uneven spatial distribution of land degradation over the catchment. Despite that the absolute values from the forward modelling are not the same as the values from the reverse modelling (Table S2) due to the differences in climatic inputs, the relative magnitude of changes in the hydrological components are close to each other.

4.3. Hydrological alteration trends in response to the observed LULC changes

The hydrological response observed from the hydrological model in section 4.2 was further quantified by the IHA method, using the results of the 2014 model. The IHA analysis based on model results indicates that there has been a continuous alteration of the hydrological variables in the Geba catchment after the occurrence of LULC changes between the different periods (Fig. 8). The magnitude of the median monthly flow between 1972 and 1989 increased by an average of 52% during the wet months while it decreased by 49% in the dry months (Fig. 8a). The reverse pattern was observed in the remaining analysis period, where the average median monthly flow of the wet months decreased by 17% and 22% and the dry months increased by 30% and 29% in the 1989–2001 and 2001–2014, respectively. With an increase of agricultural land by 42% and a decrease of natural vegetation cover by 36%, the average median monthly flow during the wet and dry months has increased and decreased by 4% and 23%, respectively. All parameters increased from 1972 to 1989 except the 7-day maxima, which decreased from 1989 to 2001. During the 2001–2014 period, the median value of all maxima parameters moderately declined (Fig. 8b). The observed changes on the annual maxima (Fig. 8b) and minima (result not presented here) suggests that the influence of LULC dynamics on the hydrological processes were significant.

The frequency and duration of low and high flow pulses were also investigated for the response of each map (Fig. 8c). The annual pulse count and their duration increased in the first period and consistently decreased in the later periods. Increasing of pulses below and above the given threshold in the first period shows that the hydrological responses in the catchment were flashier in the 1980s and 1990s. In the latter two periods (the 2000s and 2010s) the peak runoff hydrographs declined in most part of the catchment. Most importantly, the number of high and low pulses is related to the rise and fall rate which give a good understanding of how the streamflow response to catchment characteristic is increasing/decreasing. Fig. 8d shows the trend of median daily flow rising and falling rates resultant from each LULC map. Like the high and low pulse pattern, the median rise rate (positive differences between two consecutive daily values) has increased from 1.1 m^3/s in 1972 to 1.6 m^3/s in the 1989 land use and then started to decrease by 0.4 and 0.65 m^3/s from 1989 to 2001 and to 2014, respectively. In the same way, the median fall rate (negative differences) increased from 0.2 to 0.6 m^3/s in 1972 to 1989 and then decreased by 0.1 m^3/s in the latter two periods (2001 & 2014).

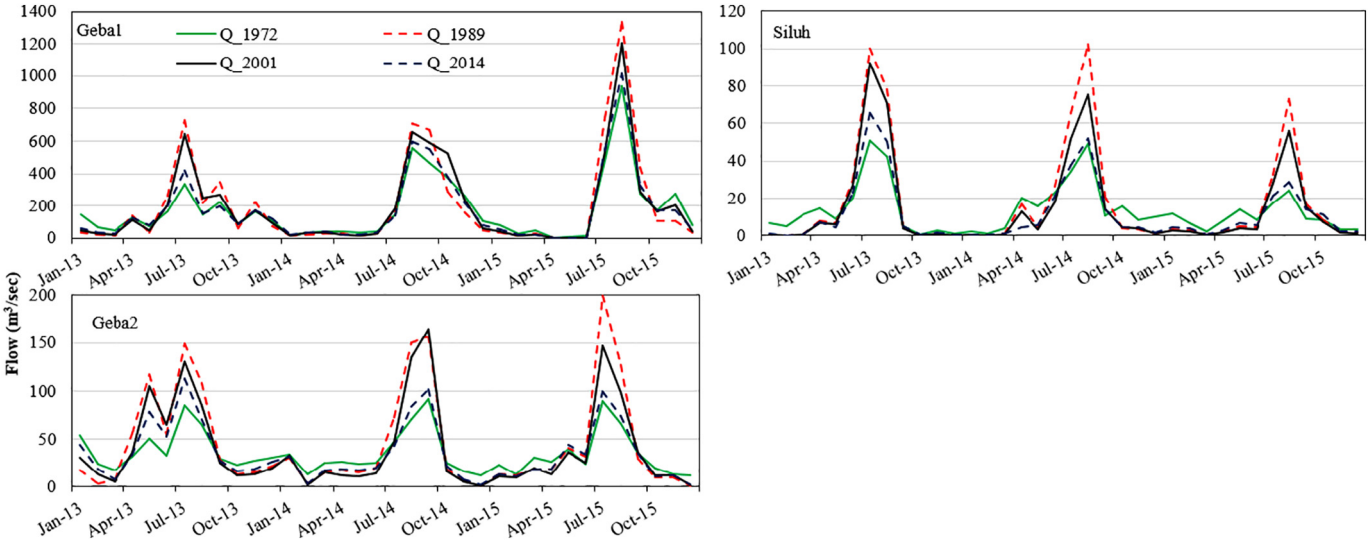

Fig. 5. Comparison of simulated streamflow in multiple sub-catchments and different LULC (1972, 1989, 2001 and 2014) using reverse modelling approaches (2014 model).

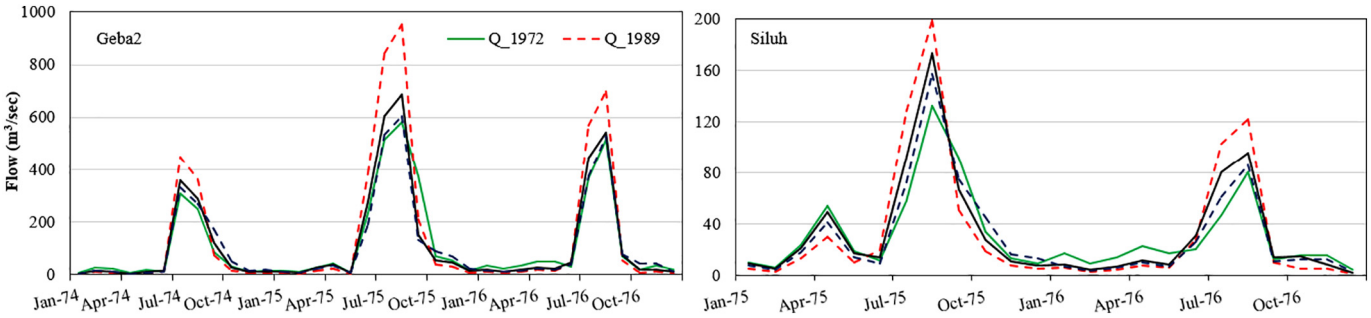

Fig. 6. Comparison of simulated streamflow in two sub-catchments and different LULC (1972, 1989, 2001 and 2014) using forward modelling approaches (1972 model).

4.4. Hydrological impacts of individual land use/land cover changes

A preliminary analysis using a pair-wise correlation matrix indicated that most LULC types have a strong association with the change in hydrological components (Table 5). Natural vegetation cover including wood and bushland have a significant negative correlation with annual and wet season flows, but a strong positive correlation with dry season flow, SWS and AET in the catchment. In contrast, the expansion of agricultural and bareland showed a significant positive correlation with annual and wet season flows and a significant negative correlation with SWS and dry season flow (Table 5). Although statistically not significant, the grassland and water body classes also showed a positive and negative effect on the different hydrological components. The significant correlation between all except grassland and water classes indicates that changes in these land use categories were the main driving force for the observed change in hydrological regimes.

The obtained values of R^2x, R^2y and Q^2_{cum} are above 0.5 which suggests a good predictive capacity of the models. A summary of three PLSR models constructed separately for streamflow, AET and SWS during the reverse modelling exercises are presented in Tables 6 and 7. The first components for streamflow, AET, and SWS accounted for 58.2, 75.4, and 97.3% of the total variance, respectively (Table 6). The addition of the second component improved the prediction error in streamflow and AET, which cumulatively explained 84.6 and 97.9% of the total variance, respectively. Further addition of third model components for the streamflow explained the total variance by 97.8% (Table 6). This notwithstanding, the addition of the second model for SWS and third PLSR model component for AET did not significantly improve the predictive capacity of the models. Prediction errors decrease with an increase in the number of components; however, adding more components can also lead to a greater prediction error, which means that the later added components may not strongly correlate with the residuals of predicted variables (Yan et al., 2016).

Table 7 presents the summary of weights and VIP of individual LULC classes. Although the weights are important to show the strength and direction of impacts, a comprehensive demonstration of the relative importance of the predictors can be explained by their VIP values. In the case of streamflow, the highest VIP value was obtained from agriculture, followed by bareland and bushland (Table 7). The streamflow appeared to increase with the expansion of agricultural and bareland, whereas the

Table 4
Mean annual (2013–2015) hydrological fluxes in (mm/year) of each LULC maps from the reverse modelling approach (2014 model) at different sub-catchments.

	Land use/cover				Change in fluxes (%)			
	1972	1989	2001	2014	1972–1989	1989–2001	2001–2014	1972–2014
Geba 1								
Annual rainfall	600	600	600	600	0	0	0	0
SWS	75	42	50	66	−44	19.0	24	−12
AET	407	332	376	434	−18	13.3	13	7
Annual flow	181	250	213	141	38	−14.8	−51	−22
Wet season flow	111	196	150	94	77	−23.5	−60	−15
Dry season flow	70	54	63	47	−30	16.7	−34	−33
Runoff coefficient	0.30	0.42	0.36	0.24	40	−14.3	−50	−20
Wet season/annual flow	0.61	0.78	0.70	0.67	28	−10.3	−4	10
Dry season/annual flow	0.39	0.22	0.30	0.33	−44	36.4	9	−15
Geba 2								
Annual rainfall	550	550	550	550	0	0	0	0
SWS	107	56	79	93	−48	41.1	15	−13
AET	328	270	329	351	−18	21.9	6	7
Annual flow	123	224	150	103	82	−33.0	−46	−16
Wet season flow	72	166	102	64	131	−38.6	−59	−11
Dry season flow	58	51	47	37	−12	−7.8	−27	−36
Runoff coefficient	0.22	0.41	0.27	0.19	86	−34.1	−42	−14
Wet season/annual flow	0.59	0.74	0.68	0.62	25	−8.1	−10	5
Dry season/annual flow	0.41	0.26	0.31	0.36	−37	19.2	14	−12
Siluh								
Annual rainfall	540	540	540	540	0	0	0	0
SWS	124	84	109	132	−32	29.8	17	6
AET	369	313	355	388	−15	13.4	9	5
Annual flow	92	165	108	72	79	−34.5	−50	−22
Wet season flow	49	142	80	34	190	−43.7	−135	−31
Dry season flow	33	23	28	16	−30	21.7	−75	−52
Runoff coefficient	0.17	0.31	0.20	0.13	82	−35.5	−54	−24
Wet season/annual flow	0.53	0.86	0.74	0.47	62	−14.0	−57	−11
Dry season/annual flow	0.36	0.14	0.26	0.22	−61	85.7	−18	−39

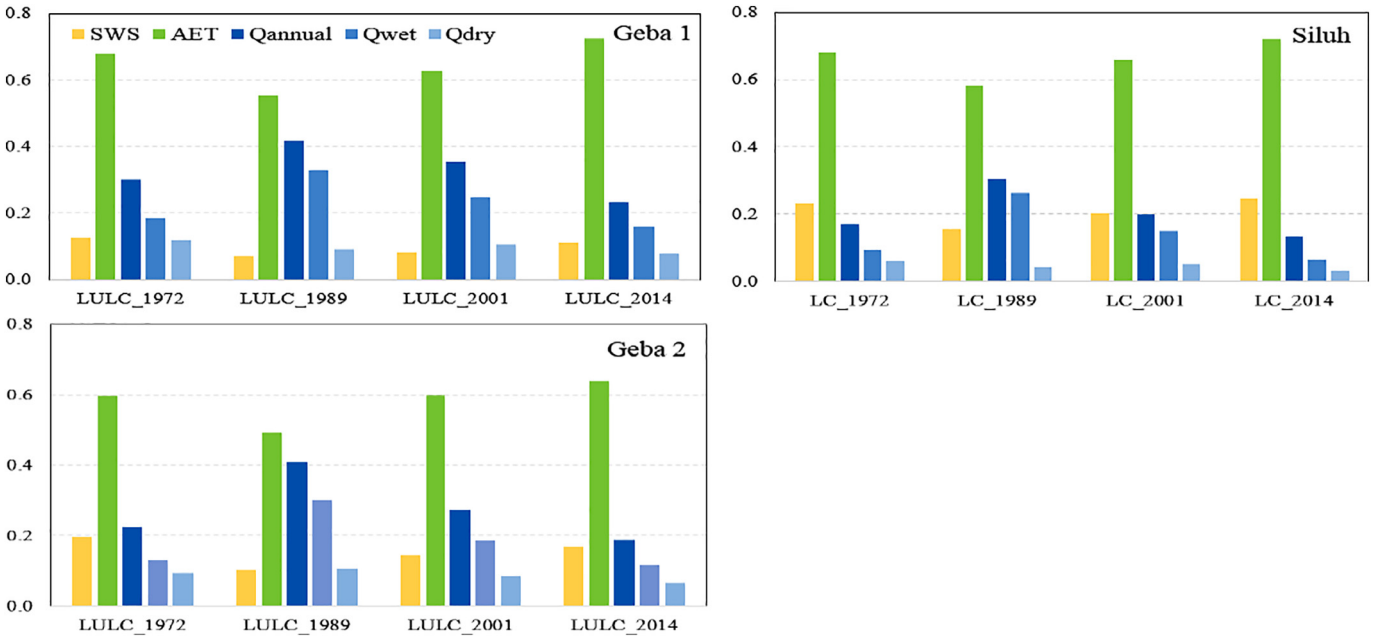

Fig. 7. Long-term change pattern of each hydrological components corresponding to the observed land use/cover change for the last 44 years.

negative values of weight indicate the natural vegetation cover, including bush, forest and woodlands contributed to a decreasing trend of streamflow in the catchment. A lower VIP value for grassland (0.79) and water body (0.81) suggests the contribution of these LULC types on the hydrological change is not significant compared to the others. Similarly, LULC types most closely associated with AET fluxes (shown by high VIP values) were bareland (1.30), bushland (1.30), and forest (1.08). However, their contribution to AET is in the opposite direction, where the AET decreases significantly with increasing of bareland but bush and forest coverages encouraged an increment (Table 7). With regard to soil water SWS, all but agriculture and water body obtained a VIP of greater than one and except bareland all LULC types contributed to an increase in SWS (Table). In summary, the PLSR model identified the main land use dynamics that have affected the change in hydrological components of the catchment. PLSR model results from the forward modelling approach show a similar pattern to the reverse modelling (Tables S9 and S10).

5. Discussion

The results from both forward and reverse hydrological modelling, IHA analysis and PLSR model demonstrated that the hydrological response in the Geba catchment has been significantly affected by the observed dynamic LULC change in the last four decades. Over the whole period (1972–2014) of analysis, the total runoff, wet and dry season flows and SWS has decreased whereas average AET over the catchment has increased. This is due to the overall net decrease in natural vegetation cover and the net increase in the agricultural land (Table 1). An

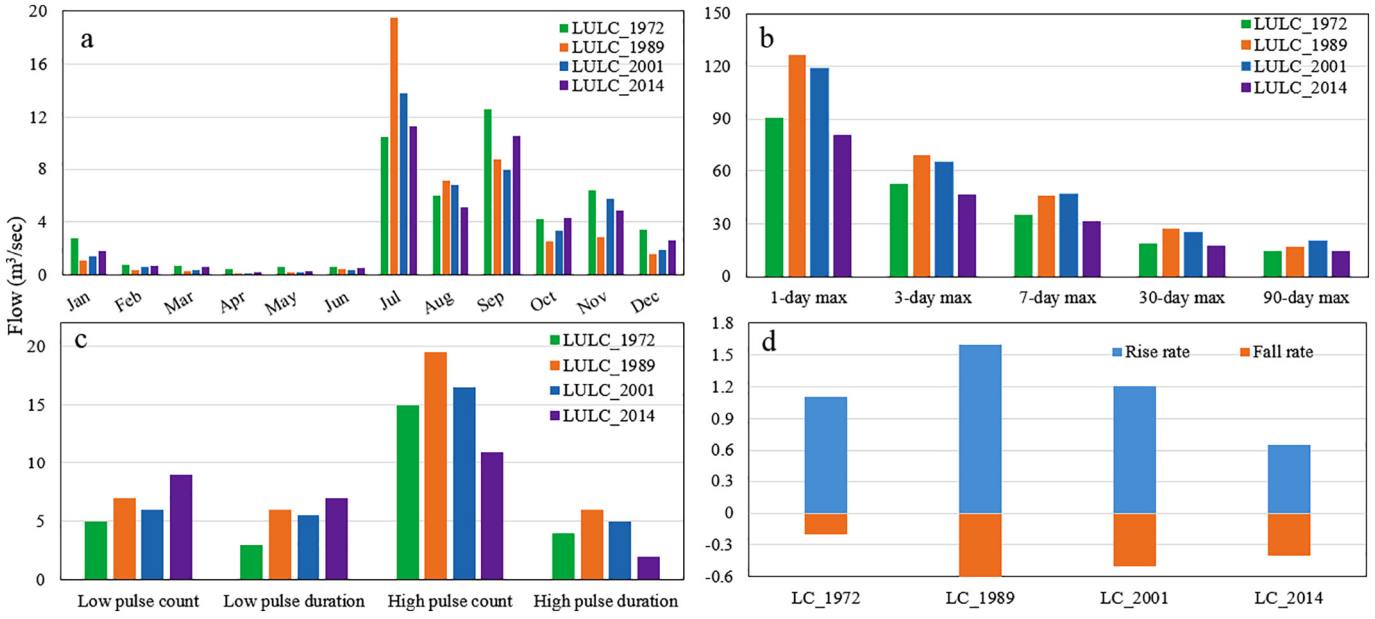

Fig. 8. Comparison of hydrological responses for each of the four LULC maps using hydrological alteration parameters: (a) Magnitude of median monthly flow; (b) Magnitude of median annual maxima flows; (c) Frequency and duration of high and low pulses; and (d) Rise and fall rate of flows.

Table 5
Pearson correlation matrices for the change in LULC types and different hydrological components (streamflow, Soil water storage, and Evapotranspiration) in Geba 1 during the reverse modelling approach and for the entire period (1972–2014).

Variables	AGRI	WOOD	FORE	BARE	WATE	BUSH	GRAS	Annual	Wet	Dry	SWS	AET
AGRI	**1**											
WOOD	−0.96	**1.00**										
FORE	−0.84	**0.95**	**1.00**									
BARE	0.16	**−0.96**	−0.64	**1.00**								
WATE	0.69	−0.48	−0.20	−0.52	**1.00**							
BUSH	**−0.98**	**0.96**	**0.96**	**−0.98**	0.48	**1.00**						
GRAS	−0.61	0.77	0.94	−0.82	0.15	**0.98**	**1.00**					
Annual	**0.95**	−0.95	−0.57	**0.98**	−0.69	**−0.97**	−0.82	**1.00**				
Wet	**0.97**	**−0.96**	−0.68	**0.98**	−0.56	**−0.97**	−0.87	**0.98**	**1.00**			
Dry	**−0.98**	**0.96**	0.41	**−0.98**	−0.63	**0.98**	0.17	0.21	−0.01	**1.00**		
SWS	**−0.98**	**0.99**	**0.96**	**−0.98**	0.15	**0.95**	**0.98**	−0.82	**−0.94**	0.30	**1.00**	
AET	−0.49	**0.97**	**0.96**	**−0.96**	0.64	**0.97**	0.84	**−0.99**	**−1.00**	−0.08	0.86	**1**

Bold values indicate a significant relationship at a level of $P < 0.05$.

increase in peak flow and a decrease in low flow during 1972–1989 are attributed to the rapid expansion of cultivable and grazing lands at the expense of natural vegetation cover between the mid-1970s to the end of 1990s. The decline in natural vegetation cover during this period (Gebremicael et al., 2018) contributed to low infiltration and canopy interception so that the incoming rainfall was converted into surface runoff.

The decrease in surface runoff and increase in SWS and AET in the 2000s and 2010s results from the notable improvement of natural vegetation cover in the 2001 and 2014 LULC maps. The detected increment in natural vegetation cover during the last two periods influenced the partitioning of incoming rainfall to contribute more evapotranspiration and enhance the infiltration capacity and resulted in a reduced surface runoff. However, the rate of increase in low flows stalled in the 2010s in most sub-catchments which might be explained by an increase in water withdrawals for irrigation. Several local studies (e.g., Alemayehu et al., 2009; Gebremeskel et al., 2018; Kifle and Gebretsadikan, 2016; Nyssen et al., 2010) reported that irrigated agriculture in the catchment has increased by >280% from 2006 to 2015. For example, irrigated agriculture in Genfel and Agulae sub-catchments (Fig. 1) has increased from 83 and 143 ha in 2006 to >643 and 946 ha in 2015, respectively.

Model parameters value for two different periods (model in the 1970s and 2010s) were also compared to infer the possible causes of changes. The differences between the values of the two model parameters (Tables S2–S6) is attributed to the modification of the basin physical characteristics. For example, parameter values of Ksat and Gash interception model (EoverR) increased from 1972 to 2014, while the values of the M parameter and the CanopyGapFraction decreased for the same period. This suggests that with an increase in natural vegetation cover more water contributed to infiltration and evapotranspiration instead of going to surface runoff. Change in model parameters between the two periods indicates a change in catchment characteristic response behaviour (Gebremicael et al., 2013; Seibert and McDonnell, 2010).

The findings of IHA and PLSR analysis are consistent with the result from the hydrologic model that expansion of agriculture and grazing land in the last four decades contributed to an increase of surface runoff and a decrease of AET and SWS in the catchment. Alteration of monthly flows during the dry and wet seasons is attributed to the dynamic LULC change of the catchment. The IHA analysis result showed that the magnitude of median annual flow maxima and minima were significantly affected by all LULC maps. The direction of change in flow rise and fall rates was in agreement with the observed LULC changes which implies that the changes in the rate and frequency of water conditions are linked to the LULC change of the catchment. Surface runoff generation showed a strong negative correlation with forest, wood and bushlands while a strong positive relationship occurred between dry season flow and these LULC types. The observed dynamic change in these LULC types during the different analysis periods inversely affected the infiltration capacity of the soil and subsequently overland flow to the streams. It is also reported in several studies (e.g., Gashaw et al., 2018; Woldesenbet et al., 2017; Yan et al., 2016) that decrease in vegetation cover contributed to an increase in surface runoff and decrease in dry season flows.

Our findings are in agreement with previous local and neighbouring basin studies. A similar decline in the dry season and increase in wet season flows was reported in the Geba2 sub-catchment. Abraha (2014) showed that the conversion of natural vegetation to agricultural crops in the upper Geba catchment (Geba2) increased surface runoff by 72% and decreased dry season flow by 32% over 1972–2003. Nyssen et al. (2010) showed that the surface runoff volume significantly reduced after catchment management interventions in My ZigZag. Descheemaeker et al. (2006) found a reduction of surface runoff by 80% after the restoration of vegetation cover in the same watershed. Similarly, Negusse et al. (2013) found that the availability of groundwater in Arbiha Weatsbiha watershed of Genfel sub-catchment increased by more than ten times from 1993 to 2013. Bizuneh (2013), in contrast, found that despite almost all land had been converted into cultivable area, surface runoff and base-flows did not change in the Siluh watershed. It is not clear why this finding disagrees with results of all other studies in this basin and other neighbouring basins. What all referred studies share is that these were based either on experimental plots or

Table 6
Summary of the PLSR models of streamflow, AET and SWS hydrological components in Geba 1 during the entire study period during the reverse modelling approach (1972–2014).

Response Y	R^2x	R^2y	Q^2	Component	% of explained variability in y	Cumulative % of explained variability in y	RMSEcv (mm)	Q^2_{cum}
Streamflow (annual, Wet & dry season flows)	0.83	0.87	0.76	1	58.2	58.2	11.3	0.87
				2	26.4	84.6	10.2	0.83
				3	**13.2**	**97.8**	**8.9**	**0.94**
AET	0.90	0.89	0.98	1	75.4	75.4	18.3	0.87
				2	**22.5**	**97.9**	**14.8**	**0.96**
SWS	0.67	0.98	0.87	1	97.3	97.3	3.6	0.87

Bold values indicate the last model component which explaines the total variance.

Table 7
Variable importance of the projection values (VIP) and PLSR for the hydrological components of Geba 1during the entire study period during the reverse modelling approach (1972–2014).

PLSR predictors	Streamflow (annual, wet and dry)				AET			SWS	
	VIP	W*(1)	W*(2)	W*(3)	VIP	W*(1)	W*(2)	VIP	W*(1)
AGRI	1.37	0.08	**0.48**	0.26	0.68	−0.05	0.25	0.93	**−0.38**
WOOD	0.90	−0.23	**−0.47**	**−0.42**	0.82	**0.40**	0.20	1.01	**0.38**
FORE	0.93	**−0.35**	0.20	−0.19	1.07	**0.63**	0.25	1.16	**0.44**
BARE	1.29	**0.51**	0.15	**−0.68**	1.30	**−0.51**	0.28	1.11	**−0.42**
WATE	0.81	−0.21	−0.28	−0.18	0.68	0.24	0.16	0.19	0.07
BUSH	1.12	**−0.51**	−0.30	−0.39	1.30	**0.52**	0.21	1.16	**0.44**
GRAS	0.79	−0.26	−0.05	**−0.33**	0.63	0.25	−0.03	1.23	**0.47**

W* > 0.3 and <−0.3 suggests PLSR components are mainly weighted on the corresponding variables.
Negative and positive values show direction of the regressions.
Bold values indicate a significance relationship at w* > 0.3 and <-0.3.

at very small watershed levels, the findings of which are difficult to extrapolate to catchment scale. The approach in this study adopted the catchment scale, and uniquely integrates hydrological simulations to identify the hydrological response of land management dynamics, detect the magnitude of the fluctuations of the simulated streamflow and then identify the contribution of each LULC type on the change in streamflow. This approach has explicitly demonstrated the impact of land management interventions on the hydrology with a better understanding at different spatial scales. The results are also consistent with several studies in the neighbouring basins which reported an increasing trend of wet season flows while the dry season flows decreased due to the conversion of natural vegetation cover into agricultural and grazing lands (Gashaw et al., 2018; Gebremicael et al., 2013; Haregeweyn et al., 2014; Tekleab et al., 2014; Woldesenbet et al., 2017). For example, Tekleab et al. (2014) and Gebremicael et al. (2013) reported that the conversion of natural vegetation cover into agricultural and bareland in the Upper Blue Nile basin has caused an increase of surface runoff and a decrease of base-flows up to 75% and 50%, respectively.

It is essential to point out one major limitation of this study: it did not quantify actual water abstractions over the study period, and therefore the observed flows at gauging stations were not naturalized. As water abstractions during the low flow season have likely significantly increased since around 2010, this must have influenced some hydrological model parameters. Naturalizing the streamflow from abstraction can improve the model and subsequently the results from this approach.

6. Conclusions

The investigation of the effect of LULC change to the hydrological flow from the Geba catchment, over the period 1972 to 2014, has shown that, the expansion of agricultural and grazing land at the expense of natural vegetation cover during the period 1972 to 1989 increased surface runoff and contributed to a decrease in dry season flow. The rate of land degradation decreased and natural vegetation started recovering from the mid-1990s due to integrated watershed management interventions which resulted in an increased dry season flows and a declined surface runoff in the period 1989 to 2001. Whereas the wet season flows generated from surface runoff continued to decline in the most recent period (2001–2014), this was accompanied by an unexpected decline in dry season flow, which may be attributed to an increase in water withdrawals for irrigation. Analysis of 33 hydrological alteration parameters of simulated hydrographs from different LULC maps showed that the change in magnitude of median monthly flow, annual extremes, frequency and duration of flow pulses and rate and frequency of water conditions were consistent with the observed LULC changes over the period considered. In summary, the rate of increase in the peak flow and decrease in the dry season flow appeared to reduce after the 2000s. This result is attributed to the improvement of natural vegetation cover through watershed management interventions in the catchment.

The key finding from this study is that most LULC types are strongly affected changes of hydrological components. Cultivation and bareland areas increase wet season flow and reduce dry season flow, AET and SWS. The reverse was found for natural vegetation cover (forest, wood and bush areas) which increases dry season flow, AET and SWS but decreases the wet season flow. The hydrological response to LULC change was more pronounced at sub-catchment level, which is mainly linked to the observed uneven spatial distribution of land degradation and rehabilitation in the catchment.

In conclusion, this paper has shown that ongoing watershed management interventions can increase dry season flows, while decreasing wet season flows. Dry season flows are of utmost importance for stakeholders as it comes when most needed. Stakeholders in the Geba catchment are already taking advantage of using some of the increased dry season flow for irrigation purposes. Further in-depth investigation of the impact of integrated watershed management intervention on the low flows is essential to understand the potential downstream implications, including in the Tekeze-Atbara sub-basin and the Nile basin as a whole.

The approach applied in this study was found to be realistic to quantify hydrological responses to a human-induced environmental change in a complex catchment. Particularly, the development of a fully distributed hydrological model in wflow_PCRaster/Python modelling framework showed a good potential to simulate all hydrological components by maximizing available spatial data with little calibration to minimize the risks associated with over-parameterization. The PLSR model could subsequently identify how specific LULC types impact the different components of the hydrological cycle.

Acknowledgements

This research was funded by The Netherlands Fellowship Programme (NFP) and The Tigray Agricultural Research Institute (TARI). The authors would like to thank the Ethiopian National Meteorological Agency and Ethiopian Ministry of Water Resources for providing hydroclimate data.

Appendix A. Supplementary data

Supplementary data to this article can be found online at https://doi.org/10.1016/j.scitotenv.2019.01.085.

References

Abdi, H., 2010. Partial least squares regression and projection on latent structure regression (PLS R). Wiley Interdiscip. Rev. Comput. Stat. 2, 97–106.
Abraha, A. Ai, 2014. Modeling hydrological responses to changes in land cover and climate in upper Geba Basin, Northern Ethiopia. PhD thesis. Freie Universität Berlin. Berlin, Germany.
Alemayehu, F., Taha, N., Nyssen, J., Girma, A., Zenebe, A., Behailu, M., Poesen, J., 2009. The impacts of watershed management on land use and land cover dynamics in Eastern Tigray (Ethiopia). Resour. Conserv. Recycl. 53, 192–198.
Ariti, A.T., van Vliet, J., Verburg, P.H., 2015. Land-use and land-cover changes in the Central Rift Valley of Ethiopia: assessment of perception and adaptation of stakeholders. Appl. Geogr. 65, 28–37.
Belay, K.T., Van Rompaey, A., Poesen, J., Van Bruyssel, S., Deckers, J., Amare, K., 2014. Spatial analysis of land cover changes in eastern Tigray (Ethiopia) from 1965 to 2007: are there signs of a Forest transition? Land Degrad. Dev. 26, 680–689.
Bizuneh, A. Abebe, 2013. Modeling the Effect of Climate and Land Use Change on the Water Resources in Northern Ethiopia: the Case of Suluh River basin. PhD Thesis. Freie Universität, Berlin, Germany.
Carver, Nash, R.H., 2009. Doing Data analysis with SPSS version 16. Cengage Learning, Belmont.
Chen, Q., Mei, K., Dahlgren, R.A., Wang, T., Gong, J., Zhang, M., 2016. Impacts of land use and population density on seasonal surface water quality using a modified geographically weighted regression. Sci. Total Environ. 572, 450–466.

Descheemaeker, K., Nyssen, J., Poesen, J., Raes, D., Haile, M., Muys, B., Deckers, S., 2006. Runoff on slopes with restoring vegetation: a case study from the Tigray highlands, Ethiopia. J. Hydrol. 331, 219–241.
Gash, J.H.C., Lloyd, C.R., Lachaud, G., 1995. Estimating sparse forest rainfall interception with an analytical model. J. Hydrol. 170, 79–86.
Gashaw, T., Tulu, T., Argaw, M., Worqlul, A.W., 2018. Modeling the hydrological impacts of land use/land cover changes in the Andassa watershed, Blue Nile Basin, Ethiopia. Sci. Total Environ. 619, 1394–1408.
Gebremeskel, G., Gebremicael, T.G., Girmay, A., 2018. Economic and environmental rehabilitation through soil and water conservation, the case of Tigray in northern Ethiopia. J. Arid Environ. 151, 113–124.
Gebremicael, T.G., Mohamed, Y.A., Betrie, G.D., van der Zaag, P., Teferi, E., 2013. Trend analysis of runoff and sediment fluxes in the Upper Blue Nile basin: a combined analysis of statistical tests, physically-based models and landuse maps. J. Hydrol. 482, 57–68.
Gebremicael, T.G., Mohamed, Y.A., van der Zaag, P., Hagos, E.Y., 2017. Temporal and spatial changes of rainfall and streamflow in the upper Tekeze–Atbara River Basin, Ethiopia. Hydrol. Earth Syst. Sci. 21, 2127–2142.
Gebremicael, T.G., Mohamed, Y.A., van der Zaag, P., Hagos, E., 2018. Quantifying longitudinal land use change from land degradation to rehabilitation in the headwaters of Tekeze-Atbara Basin, Ethiopia. Sci. Total Environ. 622-623, 1581–1589.
Gebreyohannes, T., De Smedt, F., Walraevens, K., Gebresilassie, S., Hussien, A., Hagos, M., Gebrehiwot, K., 2013. Application of a spatially distributed water balance model for assessing surface water and groundwater resources in the Geba basin, Tigray, Ethiopia. J. Hydrol. 499, 110–123.
Gyamfi, C., Ndambuki, J.M., Salim, R.W., 2016. Hydrological responses to land use/cover changes in the Olifants Basin, South Africa. Water 8, 588.
Haregeweyn, N., Tesfaye, S., Tsunekawa, A., Tsubo, M., Meshesha, D., Adgo, E., Elias, A., 2014. Dynamics of land use and land cover and its effects on hydrologic responses: case study of the Gilgel Tekeze catchment in the highlands of Northern Ethiopia. Environ. Monit. Assess. 187, 1–14.
Haregeweyn, N., Tsunekawa, A., Poesen, J., Tsubo, M., Meshesha, D.T., Fenta, A.A., Nyssen, J., Adgo, E., 2017. Comprehensive assessment of soil erosion risk for better land use planning in river basins: case study of the Upper Blue Nile River. Sci. Total Environ. 574, 95–108.
Hargreaves, G.H., Riley, J.P., 1985. Agricultural benefits for Senegal River basin. J. Irrig. Drain. Eng. 111 (2), 113–124.
Hassaballah, K., Mohamed, Y., Uhlenbrook, S., Biro, K., 2017. Analysis of streamflow response to land use and land cover changes using satellite data and hydrological modelling: case study of Dinder and Rahad tributaries of the Blue Nile (Ethiopia–Sudan). Hydrol. Earth Syst. Sci. 21, 5217.
Hengl, T., de Jesus, J.M., Heuvelink, G.B., Gonzalez, M.R., Kilibarda, M., Blagotić, A., Bauer-Marschallinger, B., 2017. SoilGrids250m: global gridded soil information based on machine learning. PLoS One 12, e0169748.
Hurkmans, R.T.W.L., Terink, W., Uijlenhoet, R., Moors, E.J., Troch, P.A., Verburg, P.H., 2009. Effects of land use changes on streamflow generation in the Rhine basin. Water Resour. Res. 45 (6).
Hurni, H., Tato, K., Zeleke, G., 2005. The implications of changes in population, land use, and land management for surface runoff in the upper Nile basin area of Ethiopia. Mt. Res. Dev. 25, 147–154.
Karssenberg, D., Schmitz, O., Salamon, P., de Jong, K., Bierkens, M.F., 2010. A software framework for construction of process-based stochastic spatio-temporal models and data assimilation. Environ. Model. Softw. 25, 489–502.
Kifle, M., Gebretsadikan, T.G., 2016. Yield and water use efficiency of furrow irrigated potato under regulated deficit irrigation, Atsibi-Wemberta, North Ethiopia. Agric. Water Manag. 170, 133–139.
Kiptala, J.K., Mohamed, Y., Mul, M.L., Van Der Zaag, P., 2013. Mapping evapotranspiration trends using MODIS and SEBAL model in a data scarce and heterogeneous landscape in eastern Africa. Water Resour. Res. 49, 8495–8510.
Kiptala, J., Mul, M., Mohamed, Y., Van der Zaag, P., 2014. Modelling stream flow and quantifying blue water using a modified STREAM model for a heterogeneous, highly utilized and data-scarce river basin in Africa. Hydrol. Earth Syst. Sci. 18, 2014.
Köhler, L., Mulligan, M., Schellekens, J., Schmid, S., Tobón, C., 2006. Hydrological impacts of converting tropical montane cloud forest to pasture, with initial reference to northern Costa Rica. Final Technical Report DFID-FRP Project no. R799.
Li, H., Sivapalan, M., 2011. Effect of spatial heterogeneity of runoff generation mechanisms on the scaling behavior of event runoff responses in a natural river basin. Water Resour. Res. 47, W00H08.
Mathews, R., Richter, B.D., 2007. Application of the indicators of hydrologic alteration software in environmental flow setting. JAWRA 43, 1400–1413.
Moriasi, D.N., Arnold, J.G., Van Liew, M.W., Bingner, R.L., Harmel, R.D., Veith, T.L., 2007. Model evaluation guidelines for systematic quantification of accuracy in watershed simulations. Trans. ASABE 50, 885–900.
Negusse, T., Yazew, E., Tadesse, N., 2013. Quantification of the impact of integrated soil and water conservation measures on groundwater availability in Mendae catchment, Abraha We-Atsebaha, eastern Tigray, Ethiopia. Momona Ethiopian J. Sci. 5, 117–136.
Nyssen, J., Vandenreyken, H., Poesen, J., Moeyersons, J., Deckers, J., Haile, M., Govers, G., 2005. Rainfall erosivity and variability in the Northern Ethiopian Highlands. J. Hydrol. 311, 172–187.
Nyssen, J., Clymans, W., Descheemaeker, K., Poesen, J., Vandecasteele, I., Vanmaercke, M., Haregeweyn, N., 2010. Impact of soil and water conservation measures on catchment hydrological response—a case in north Ethiopia. Hydrol. Process. 24, 1880–1895.
Nyssen, J., Frankl, A., Haile, M., Hurni, H., Descheemaeker, K., Crummey, D., Ritler, A., Portner, B., Nievergelt, B., Moeyersons, J., 2014. Environmental conditions and human drivers for changes to north Ethiopian mountain landscapes over 145 years. Sci.Total Environ. 485, 164–179.
Oliver, M.A., Webster, R., 1990. Kriging: a method of interpolation for geographical information systems. Int. J. Geogr. Inf. Sci. 4, 313–332.
Ott, B., Uhlenbrook, S., 2004. Quantifying the impact of land-use changes at the event and seasonal time scale using a process-oriented catchment model. Hydrol. Earth Syst. Sci. 8, 62–78.
Saraiva-Okello, A.M.L., Masih, I., Uhlenbrook, S., Jewitt, G.P.W., van der Zaag, P., Riddell, E., 2015. Drivers of spatial and temporal variability of streamflow in the Incomati River basin. Hydrol. Earth Syst. Sci. 19, 657–673.
Savenije, H., 2010. HESS opinions "Topography driven conceptual modelling (FLEX-Topo)". Hydrol. Earth Syst. Sci. 14 (12), 2681–2692.
Savenije, H.H., Hoekstra, A.Y., Van der Zaag, P., 2014. Evolving water science in the Anthropocene. Hydrol. Earth Syst. Sci. 18, 319–332.
Schellekens, J., 2014. Wflow, a flexible hydrological model. OpenStream wflow documentation release 1.0 RC1, Deltares, Delft, The Netherlands.
Seibert, J., McDonnell, J.J., 2010. Land-cover impacts on streamflow: a change-detection modelling approach that incorporates parameter uncertainty. Hydrol. Sci. J. 55, 316–332.
Shapiro, S.S., Wilk, M.B., 1965. An analysis of variance test for normality (complete samples). Biometrika 52, 591–611. https://doi.org/10.2307/2333709.
Shi, W., Yu, X., Liao, W., Wang, Y., Jia, B., 2013. Spatial and temporal variability of daily precipitation concentration in the Lancang River basin, China. J. Hydrol. 495, 197–207.
Sivapalan, M., Blöschl, G., Zhang, L., Vertessy, R., 2003. Downward approach to hydrological prediction. Hydrol. Process. 17, 2101–2111.
Taniguchi, M., 2012. Subsurface Hydrological Responses to Land Cover and Land Use Changes. Springer Science & Business Media, Utrecht, The Netherlands.
Tekleab, S., Mohamed, Y., Uhlenbrook, S., Wenninger, J., 2014. Hydrologic responses to land cover change: the case of Jedeb mesoscale catchment, Abay/Upper Blue Nile basin, Ethiopia. Hydrol. Process. 28, 5149–5161.
Tenenhaus, M., 1998. La régression PLS, théorie et pratique. Editions Technip, Paris, France.
Tesfaye, S., Birhane, E., Leijnse, T., van der Zee, S.E.A.T.M., 2017. Climatic controls of ecohydrological responses in the highlands of northern Ethiopia. Sci. Total Environ. 609, 77–91.
Uhlenbrook, S., Roser, S., Tilch, N., 2004. Hydrological process representation at the mesoscale: the potential of a distributed, conceptual catchment model. J. Hydrol. 291, 278–296.
Vertessy, R.A., Elsenbeer, H., 1999. Distributed modeling of storm flow generation in an Amazonian rain forest catchment: effects of model parameterization. Water Resour. Res. 35, 2173–2187.
Wang, X., Zhang, J., Babovic, V., 2016. Improving real-time forecasting of water quality indicators with combination of process-based models and data assimilation technique. Ecol. Indic. 66, 428–439.
Wang, Y., Liu, Y., Jin, J., 2018. Contrast effects of vegetation cover change on evapotranspiration during a revegetation period in the Poyang Lake Basin, China. Forests 9 (4), 217.
Woldesenbet, T.A., Elagib, N.A., Ribbe, L., Heinrich, J., 2017. Hydrological responses to land use/cover changes in the source region of the Upper Blue Nile Basin, Ethiopia. Sci. Total Environ. 575, 724–741.
Wondie, M., Schneider, W., Melesse, A., Teketay, D., 2011. Spatial and temporal land cover changes in the Simen Mountains National Park, a world heritage site in North-Western Ethiopia. Remote Sens. 3, 752–766.
Yan, B., Fang, N., Zhang, P., Shi, Z., 2013. Impacts of land use change on watershed streamflow and sediment yield: an assessment using hydrologic modelling and partial least squares regression. J. Hydrol. 484, 26–37.
Yan, R., Gao, J., Li, L., 2016. Modeling the hydrological effects of climate and land use/cover changes in Chinese lowland polder using an improved WALRUS model. Hydrol. Res. 47 (S1), 84–101.
Yu, Y., Zhang, H., Singh, V.P., 2018. Forward prediction of runoff data in data-scarce basins with an improved ensemble empirical mode decomposition (EEMD) model. WaterSA 10, 388.
Zeleke, G., Hurni, H., 2001. Implications of land use and land cover dynamics for mountain resource degradation in the northwestern Ethiopian highlands. Mt. Res. Dev. 21, 184–191.